Article type: Original research

Manuscript title:

Prediction of Gemcitabine sensitivity in resectable Pancreatic Cancer using a Glycation Stress Transcriptomic Signature.

Short title

MG-stress classifier for PDAC sensitivity to gemcitabine.

List of authors

Oier Azurmendi Senar[1], Kosta Stosic[1], Christelle Bouchart[1,2], Julie Navez[1,3], Jawad Tarfouss[1], Rebekah Crake[4,5,6], Laurine Verset[7], Pieter Demetter[1], Marjorie Mauduit[8], Thierry Conroy[9], Jérôme Cros[10,11], Remy Nicolle[10,] Vincent Detours[12], Akeila Bellahcène[4 §], Tatjana Arsenijevic[1,13§] and Jean-Luc Van-Laethem[1,13§]; the PRODIGE-24/CCTG PA6 consortium; the MOSAPAC consortium.

[§]Authors contributed equally

[1]Laboratory of Experimental Gastroenterology, Université Libre de Bruxelles, Route de Lennik 808, 1070 Brussels, Belgium.

oier.azurmendi@ulb.be

[2]Department of Radiation Oncology, HUB Institute Jules Bordet, Université Libre de Bruxelles, Rue Meylenmeersch 90, 1070 Brussels, Belgium.

[3]Department of Hepato-biliary-pancreatic surgery, Erasme University Hospital, Université Libre de Bruxelles, Brussels, Belgium.

[4] Metastasis Research Laboratory, GIGA-Cancer, GIGA Institute, University of Liège, Belgium.

[5] Olivia Newton-John Cancer Research Institute, Melbourne, Victoria, Australia.

[6] La Trobe University School of Cancer Medicine, Melbourne, Victoria, Australia

[7] Department of Pathology, HUB Bordet Erasme Hospital, Université Libre de Bruxelles, Rue 21 Meylenmeersch 90, 1070 Brussels, Belgium.

[8] R&D Unicancer, Paris, France.

[9] Medical Oncology Department, Institut de Cancérologie de Lorraine, 54519 Vandoeuvre-lès-Nancy, France and Université de Lorraine, Inserm INSPIIRE, 54000, Nancy, France.

[10] Université Paris Cité, Centre de Recherche sur l'Inflammation (CRI), INSERM, U1149, CNRS, ERL 8252, F-75018 Paris, France.

[11] Université Paris Cité, Department of Pathology, FHU MOSAIC, Beaujon/Bichat University Hospital (AP-HP), Paris, France.

[12] Institute of Interdisciplinary Research (IRIBHM) Jacques E. Dumont, Université Libre de Bruxelles, Brussels, Belgium.

[13] Department of Gastroenterology, Hepatology and Digestive Oncology, HUB Bordet Erasme Hospital, Université Libre de Bruxelles, Route de Lennik 808, 1070 Brussels, Belgium.

Acknowledgments

We thank Unicancer and MOSAPAC consortiums for providing PRODIGE-24/CCTG PA6 clinical data.

Context Summary

Key Objective

Can metabolic gemcitabine (GEM) resistant inducer methylglyoxal stress be used to predict resistance to adjuvant GEM through a transcriptomic signature?

Knowledge Generated

The transcriptomic MG-GEM signature demonstrated the ability to distinguish between GEM sensitive and GEM resistant patients in the internal cohorts from Erasme University Hospital. MG-GEMs predictive capacity was further validated in the independent PRODIGE-24/CCTG PA6 clinical trial data. When compared to the established GemPred transcriptomic signature, MG-GEM exhibited an independent predictive behaviour. Moreover, combining both independent signatures enhanced the identification of GEM sensitive and GEM resistant patient subgroups. This combined approach may be particularly valuable in identifying patient subsets with treatment-specific responses.

Abstract

Purpose

Pancreatic ductal adenocarcinoma (PDAC) remains one of the most aggressive malignancies, largely due to chemoresistance arising from prominent cellular heterogeneity and a complex tumor microenvironment. Given this challenge, understanding the mechanisms of driving chemoresistance is essential for guiding our chemotherapeutic choice. Emerging evidence suggests that methylglyoxal (MG), a reactive glycolytic byproduct, may play a role in modulating tumor behavior and therapy response, offering a novel angle for patient stratification. Our recent study indicates that the accumulation of MG in PDAC cells leads to MG-induced cellular stress associated with gemcitabine (GEM) resistance. The primary objective of this study was to identify a predictive transcriptomic signature associated with MG stress in PDAC and compare it to the recently reported GemPred signature.

Patients and methods

MG stress classification was applied to the Puleo et al. cohort (n=309), enabling differential gene expression analysis and the development of a prognostic 16-gene MG-GEM signature through LASSO Cox regression. The signature was validated for survival prediction and diagnostic performance using cross-validation and ROC analysis.

Results

The prognostic significance and predictive performance of the signature were validated in both internal and external cohorts, including this from the phase III PRODIGE-24/CCTG PA6 trial, composed of 167 GEM and 183 FOLFIRINOX (mFFX) patients. Importantly, the MG-GEM signature demonstrated independent and complementary predictive value relative to GemPred.

Conclusion

We present a novel clinically actionable 16-gene transcriptomic signature reflecting MG-induced stress that enables robust stratification of PDAC patients likely to benefit from adjuvant GEM therapy. This model supports the development of personalized treatment strategies in pancreatic cancer.

Introduction

Pancreatic ductal adenocarcinoma (PDAC), a cancer expected to become the second leading cause of cancer-related death by 2030 [1], is known for its aggressive nature, with a 5-year overall survival (OS) rate of less than 12% [2]. Progress in developing more effective chemotherapy (CT) regimens has been slow [3], [4], [5] and to date, clinical trials involving immunotherapy and targeted therapies have largely failed, resulting in little change to current clinical practice [6], [7]. Nowadays, two main CT regimens have demonstrated their efficacy in PDAC management: full dose or modified FOLFIRINOX (folinic acid, 5-fluorouracil, irinotecan and oxaliplatin) (mFFX) and GEM combined with albumin-bound (nab) paclitaxel (GEM/Nab-P) [8]. Both regimens have globally close efficacy, while selecting GEM-based vs FFX regimens mainly rely on clinical criteria.

Gemcitabine is a deoxycytidine analogue that requires cellular uptake and intracellular phosphorylation to effectively inhibit DNA synthesis. However, its anti-proliferative and pro-apoptotic effects have limited long-term efficacy in most PDAC patients, as initially sensitive tumors often develop resistance to chemotherapy over time.

Previous studies have shown that high protein levels of GEM transporters Human Equilibrative Nucleoside Transporter 1 (hENT1) and the activating enzyme Deoxycytidine Kinase (dCK), GEM activating enzymes, are associated with longer survival [9]. Furthermore, recent studies on primary cell cultures and patient-derived xenografts have led to the identification of transcriptomic signatures, highlighting their potential to improve treatment outcomes [10], [11].

In PDAC, growing evidence links both pathogenesis and therapy resistance to metabolic reprogramming, including adaptations such as hypoxia [12] and enhanced glycolysis [13], [14]. Glycolysis, in particular, significantly contributes to the spontaneous generation of methylglyoxal (MG) [15], a highly reactive dicarbonyl compound that glycates proteins, lipids and nucleic acids, creating MG-adducts. MG-induced cellular stress has been widely studied in the initiation of diabetes and its microvascular complications [16]. Glycation stress characterized by the accumulation of MG-adducts is now recognized as a common feature in human cancers, including colon [17], breast [18] and PDAC [19]. In colorectal tumors, glycolytic activity and the intrinsic resistance of KRAS-mutated cells to EGFR-targeted therapy have been observed. This resistance was reduced with carnosine, a potent scavenger of MG, highlighting the therapeutic potential of targeting MG stress in cancer [20]. Moreover, it has been demonstrated that, when maintained at sub-cytotoxic levels through glyoxalases detoxification enzymes (GLO1 and GLO2), MG not only promotes tumor growth but also impairs the efficacy of various anticancer treatments [21].

In our recent work, we identified a strong association between acquired GEM resistance, the heat-shock response (HSR) and MG stress occurrence in glycolytic

PDAC human samples [19]. Specifically, we demonstrated that MG stress is elevated in GEM-treated PDAC patients compared to untreated ones and this elevation is associated with poorer clinical outcomes [19]. Using PDAC models with acquired GEM resistance, we showed that MG propels cell survival and GEM tolerance through the regulation of HSR [19]. Finally, we proposed the use of MG scavengers, such as metformin and aminoguanidine, to mitigate possible consequences of glycolytic rewiring on GEM resistance.

This study aimed to identify a specific MG-stress-related signature, which we named MG-GEM, capable of stratifying patients with distinct molecular and metabolic features. We characterized the clinical and therapeutic implications of the MG-GEM signature using both internal and external cohorts. Importantly, we validated the predictive value of MG-GEM in patients treated with adjuvant GEM after PDAC resection, as opposed to those treated with FOLFIRINOX (FFX), including data from the PRODIGE 24/CCTG PA6 trial.

Materials and Methods

Patient cohorts

This study included 309 patients with pancreatic ductal adenocarcinoma (PDAC) from the French Belgian Consortium Puleo et al. cohort [22], for which comprehensive clinical annotations and microarray-based transcriptomic data were available. All patients had undergone curative-intent surgical resection, and a subset received adjuvant chemotherapy. A part of this cohort served as the discovery dataset (n=89) for deriving the MG-GEM signature and the rest of the cohort was used as validation cohort (n=220). The Puleo validation cohort was subsequently divided into two subsets: the GEM adjuvant chemotherapy (AT) group, comprising 113 patients who received adjuvant treatment, and the NoAT group, consisting of 71 patients who did not receive adjuvant therapy following tumor resection.

An additional retrospective cohort coming from monocentric Erasme University Hospital was used in this study, including 42 upfront resected localized PDAC that received GEM based chemotherapy as adjuvant treatment. All patients had surgery between 2011 and 2020 and archived formalin-fixed paraffin-embedded (FFPE) tumor specimens from surgery were available and were used for transcriptome profiling as described in [23] . The main inclusion criteria were patients of age ≥ 18 with complete clinicopathological data available and no evidence of metastatic disease prior to surgery. The main clinical exclusion criteria were a tumor histology other than a ductal adenocarcinoma and patients who died from postoperative complications within 30 days after surgery. Most patients received adjuvant chemotherapy, in line with standard clinical practice during that period. Detailed clinical follow-up and survival

data were available, allowing assessment of the prognostic and predictive value of the MG-GEM signature.

For external validation, the PRODIGE24/CCTG PA6 phase III trial cohort (n=350) was used (EudraCT: 2011-002026-52)[24]. PRODIGE-24/CCTG PA6 trial is a prospective, randomized clinical trial comparing modified FOLFIRINOX (mFFX) versus gemcitabine as adjuvant therapy in resected PDAC. This cohort provided a robust dataset to evaluate the predictive specificity of the MG-GEM signature in relation to gemcitabine response, compared to FOLFIRINOX-treated patients.

Data acquisition and processing

Affymetrix HGU219 RNA microarrays data set (n = 309) from Puleo et al. RMA-normalized probe intensities were used as the discovery cohort [22]. Gene counts were normalized by an Upper Quartile procedure and logged on a base 2 in the PRODIGE-24/CCTG PA6 [3] dataset.

Transcriptomic profile process and analysis

Crake et al. [19] MG stress classification was applied in the Puleo cohort [22] (n=309) allowing to classify the tumor according to the MG stress high (n=45) or low (n=44) status. Differential gene expression (DGE) analysis was performed between patients with different MG-stress status using the R-packages edgeR v3.40.2 and limma v3.54.2 packages [25], [26]. Genes were considered differentially expressed when log two-fold change was at least ±1 and p-adjusted value < 0.05. The Pancreatic Adenocarcinoma Molecular Gradient (PAMG) classifier was applied to determine the aggressiveness of the samples [27].

Construction of MG-GEM signature

Samples used for DGE analysis were randomly separated into a training set (75%) and testing set (25%). Least Absolute Shrinkage and Selection Operator (LASSO) penalized Cox regression was conducted using the glmnet v4.1-8 package [28]. The RMA-normalized expression values of the differentially expressed genes (DEG) of the training cohort were used as input to fit the LASSO Cox regression model with the OS as response variable. The survival v3.5-3 package was used to create the survival object, which acted as response variable. Parameter alpha was indicated as 1 to ensure the application of the lasso penalty. The goal of this model was to extract the genes with a prognostic impact that were differentially expressed across MG-stress groups by constructing a penalty function to the residual sum of squares (RSS), which was then multiplied by the regularization parameter lambda (λ). The level of the regularization of the model is controlled by the hyperparameter lambda (λ) value that balances the bias and variance in the resulting coefficients.

Henceforth, coefficient β values were obtained to identify the optimal genes using the 10-fold cross-validation. Based on the risk score of each sample, the cohort was

divided into two groups (low-risk with 0–50% vs high-risk with 50–100%). The diagnostic value of these genes was evaluated using receiver operating characteristic (ROC) curves.

Statistical analysis

Descriptive statistics are used to report patient characteristics for the MG-GEM groups. Counts and percentages are presented in each category of the categorical variables. Frequencies were compared between groups with Fisher's exact test or Pearson's Chi-squared test, depending on the expected numbers. The descriptive analyses were performed using gtsummary v1.7.2 package.

Survival analyses were conducted using the survival v3.5-3 and survminer v0.4.9 packages. Log-rank test was used to calculate the differences in Kaplan-Meier curves and p-values < 0.05 were considered as statistically significant. Multivariate Cox proportional hazard regression models were applied for survival with a 95% confidence interval. OS was defined as the time in months from diagnosis to death. Disease-free survival (DFS) was defined as the time from diagnosis to the first documentation of recurrent disease following surgery.

Non-parametric Wilcoxon test in R v4.2.3 and RStudio v2023.3.0.386 environments was used for transcriptomic data analysis, assessing significant differences in treatments in PAMG and genes expression with p values < 0.05 considered statistically significant. Statistical analysis between groups were performed by the package ggpubr v0.6.0. [29], [30].

Results

Identification of a 16-genes signature and clinicopathological correlation

Patients from the Puleo cohort (n=309 samples) [22] were classified into high (n=44) and low (n=45) MG stress tumors by applying the classification of Crake et al. [19] (Figure 1-A), which is based in the combination of expression values of 10 glycolytic genes with the expression of GLO1, the main MG detoxifying enzyme. Differential gene expression (DGE) analysis identified 365 DEGs between high and low MG stress groups (Figure 1). From those DEGs, the genes with the greatest impact on prognosis were identified using a LASSO Cox regression model applied to the OS (Supplementary Figure 1-A). The regularization hyperparameter lambda (λ) was selected using a ten-fold cross-validation and by identifying the λ with the minimum cross-validated error. (Supplementary Figure 1-B). Finally, 16 genes (FAM162A, SEC61G, NT5E, TREM1, SLC3A1, CALB2, TFF1, SLC11A1, PDIA2, PADI1, ADH1C, FXYD3, SCEL, ECT2, TIPARP and IGHG1) with non-zero coefficients were identified (Supplementary Table 1). The final risk score was defined by the expression level of

each selected gene and the coefficients obtained. Based upon the median risk scores of the discovery cohort, the patients were divided into MG-GEM high (n=43) and low (n=42) groups (Figure 2-A). The accuracy of the predictive survival model based on 16 selected genes was confirmed by the area under the curve (AUC at 2 years=0.854, AUC at 4 years=0.778, AUC at 6 years= 0.753) (Supplementary Figure 1-C).

Analysis of clinicopathological features revealed a significant association between MG-GEM status and perineural invasion (*High MG-GEM: 85%, Low MG-GEM: 66%, p = 0.040*) (Table 1).

A significant association between MG-GEM classification and clinical outcomes was confirmed in the Puleo et al. discovery cohort (Figure 2-A). Patients in the high MG-GEM group had significantly shorter OS (11.7 vs. 27.2 months, $p < 0.0001$) and DFS (7.6 vs. 17.8 months, $p < 0.0001$) compared to those in the low MG-GEM group (Figure 2-B, 2-C).

To assess the independent prognostic value of MG-GEM, a multivariate Cox proportional hazards model was constructed, including clinicopathological variables significantly associated with OS and DFS. Histological grade, perineural invasion status, and Puleo subtype, along with MG-GEM, were included in the OS model. MG-GEM remained an independent prognostic factor (*stratified HR 3.5 [95% CI 1.7 to 7.3], p= <0.001)* (Figure 2-D).

Molecular and Transcriptomic Profiling Reveals Distinct Tumor Features Associated with MG-GEM

To characterize the molecular landscape associated with MG-GEM stratification, the distribution of key mutations (KRAS, TP53, SMAD4, CDKN2A) across MG-GEM groups was evaluated. KRAS G12A mutation was more frequent in the high MG-GEM group (59% vs. 33%), while the G12V mutation was more prevalent in the low MG-GEM group (53% vs. 22%) (Table 2). Moreover, nonsense mutations in SMAD4 were significantly more common in the high MG-GEM group (25% vs. 7.9%, $p = 0.049$) (Table 2). When we applied several established transcriptomic subtype classifiers (Table 2) [22],[31],[32], high MG-GEM tumors were predominantly classified into subtypes associated with a worse prognosis. According to the Puleo classification, high MG-GEM tumors were primarily classified as Pure Basal-Like (*High MG-GEM: n=8 [20%]; Low MG-GEM: n=1 [2.7%]*) and Stroma Activated (*High MG-GEM: n=15 [38%]; Low MG-GEM: n=5 [14%]),* while the low MG-GEM group was mostly classified as Immune Classical (*High MG-GEM: n=1 [2.5%]; Low MG-GEM: n=12 [32%]).*

Surprisingly, despite the significant prognostic differences, Desmoplastic (*High MG-GEM: n=10 [25%]; Low MG-GEM: n=6 [16%])* and Pure Classical (*High MG-GEM: n=6 [15%]; Low MG-GEM: n=13 [35%]*) subtypes were found across both groups. In

accordance with the results obtained with Puleo classification, Bailey et al. profiling classified low MG-GEM tumors as immunogenic (*High MG-GEM: n=1 [2.3%]; Low MG-GEM: n=6 [14%])* and progenitor *(High MG-GEM: n=5 [12%]; Low MG-GEM: n=20 [48%]*), whereas high MG-GEM tumors were predominantly classified as squamous (*High MG-GEM: n=29 [67%]; Low MG-GEM: n=4 [9.5%]).*

Analysis of the Moffitt et al. stromal classification revealed that most high MG-GEM tumors had an activated stroma (*High MG-GEM: n=29 [67%]; Low MG-GEM: n=18 [43%]*), whereas tumors with a normal stroma were primarily classified as low MG-GEM (*High MG-GEM: n=1 [2.3%]; Low MG-GEM: n=8 [19%])* (p=0.014) (Table 2), while, no significant differences were observed between basal *(High MG-GEM: n=25 [58%]; Low MG-GEM: n=21 [50%])* and classical *(High MG-GEM: n=18 [42%]; Low MG-GEM: n=21 [50%])* Moffitt tumor subtypes (p=0.45). However, a significant difference was found when applying the dichotomous PurIST classification, with basal tumors being more common in the high MG-GEM group (*High MG-GEM: n=13 [33%]; Low MG-GEM: n=3 [8.1%])* and classical tumors more common in the low MG-GEM group (*High MG-GEM: n=27 [68%]; Low MG-GEM: n=34 [92%])* (p=0.008) (Table 2).

This molecular distinction between MG-GEM groups was further explored using the PAMG, a continuous transcriptomic score that reflects tumor aggressiveness. PAMG scores were significantly higher in low MG-GEM tumors (p=2.4e-06), supporting their association with a less aggressive tumoral phenotype (Supplementary Figure 1-D).

MG-GEM predicts survival in patients having received adjuvant GEM

To assess the prognostic relevance of the MG-GEM signature, we applied it to multiple independent cohorts. First, MG-GEM stratification was performed in the remaining samples from the Puleo cohort (n=211) which were initially excluded for being classified as medium glycolytic (Figure 3-A). Kaplan–Meier survival analysis was conducted and showed significantly lower OS (p=<0.001) (Figure 3-B) and DFS (p=<0.001) (Figure 3-C) in the high MG-GEM group (n=106), thereby confirming the signature's prognostic value. Next, we validated these findings in our newly established monocentric Erasme University Hospital cohort (n=42) [30], an independent retrospective series of GEM AT patients with resected PDAC (Figure 3-D). Consistent with previous results, patients in the high MG-GEM group had significantly reduced OS (p=0.0025) (Figure 3-E) and DFS (p=0.05) (Figure 3-F); further reinforcing the clinical relevance of the MG-GEM as a prognostic biomarker.

Given the previously established link between MG stress and GEM chemoresistance, we next assessed if MG-GEM was predictive of GEM sensitivity. We tested the expression of several genes with specific roles in GEM metabolism. The low MG-GEM group showed higher expression levels of concentrative nucleoside transporter 1

(CNT1), a critical transporter for GEM cell uptake (p=0.0099). In contrast, the high MG-GEM group showed elevated expression of two enzymes associated with GEM resistance: ribonucleotide reductase catalytic subunit M1 (RRM1) (p=0.047), and cytidine deaminase (CDA) (p=4.9e-05), which contribute to GEM inactivation and DNA synthesis bypass (Supplementary Figure 2).

Next, we applied the MG-GEM signature on 2 subsets of the Puleo validation cohort (Figure 4-A): GEM adjuvant chemotherapy (AT) subset, consisting of 113 patients who received GEM as AT and a second subset, called NoAT, consisting of 71 patients that did not receive adjuvant therapy post tumor resection. Among patients who received adjuvant GEM, MG-GEM low patients had significantly higher OS (p=0.009) (Figure 4-B) and DFS (p=0.012) (Figure 4-C) than patients classified as MG-GEM high. No significant differences of OS (p=0.22) (Supplementary Figure 3-A) and DFS (p=0.43) (Supplementary Figure 3-B) were observed between the MG-GEM subgroups that did not receive adjuvant GEM.

To evaluate the treatment specificity of the MG-GEM signature, we next analyzed the PRODIGE-24/TGCC PA6 cohort, which includes 183 patients treated with adjuvant FOLFIRINOX (FFX) and 167 patients treated with adjuvant gemcitabine (GEM) (Figure 4-D), as previously described [10]. In patients that received GEM as adjuvant therapy, the MG-GEM signature was capable of stratifying patients by OS (p=0.0017) (Figure 4-E) and DFS (p=0.0038) (Figure 4-F). Conversely, MG-GEM could not stratify patients by OS (p=0.66) and DFS (p=0.82) when applied to those receiving adjuvant FFX (Figure 4-E,F), suggesting that MG-GEM is specifically predictive for GEM therapy but not for FFX.

Independent and Complementary Predictive Value of MG-GEM and GemPred Signatures

The following step was to compare the MG-GEM predictive signature with GemPred transcriptomic signature (Figure 5-A) [10]. The observation of independence between MG-GEM and GemPred (OR=0.698, p=0.314) (Figure 5-B) enabled the combination of the signatures. When applied within GEM AT samples stratified by the GemPred classifier, MG-GEM showed prognostic relevance for OS in both GemPred+ (OS: p=0.029; Figure 5-C) and GemPred− (OS: p=0.041; Figure 5-D) subgroups. However, the lack of statistical significance for DFS in both groups (Supplementary Figure 4) suggests that the prognostic impact of MG-GEM and GemPred combined may be more robust for OS than for DFS.

Discussion

GEM is considered as one of the key drugs in the therapeutic management of PDAC tumors. Although it is effective in some patients, many tumors rapidly develop resistance, severely limiting its efficacy [33]. The molecular mechanisms underlying

chemoresistance are still debated and the strategies to improve the efficacy in PDAC treatment remain limited.

Glycolytic metabolism has been closely associated with chemotherapy resistance and poor outcome in PDAC [34], [35]. Aberrant activation of the KRAS pathway, a hallmark of PDAC, drives glucose uptake and metabolism by upregulating GLUT1 and key enzymes involved in aerobic glycolysis [36], [37]. More recently, a mechanism of GEM resistance was identified in PDAC models, wherein enhanced glycolytic flux fuels de novo pyrimidine biosynthesis, reducing GEM efficacy by creating a competitive metabolic environment [12]. GEM-resistant cells exhibited elevated levels of metabolites upstream of dihydroxyacetone phosphate and glyceraldehyde 3-phosphate [12], two known precursors of MG [12]. Furthermore, GEM treatment induces the accumulation of MG-adducts, and cells adapt to MG stress by upregulating GLO1 expression, a key MG-detoxifying enzyme [19].

These findings indicate the biological relevance of MG stress in GEM resistance and underline the importance of finding a MG stress-related gene signature.

To develop a patient's MG-GEM signature based on DEG expression linked to MG stress, Cox regression was combined with the LASSO algorithm, categorizing patients into high and low MG-GEM groups. The effectiveness of this tool in identifying populations with poorer prognosis was validated by significant results across the PAMG molecular gradient, as well as OS and DFS analyses applied not only to 2 internal validation cohorts but also to the external, independent PRODIGE-24/CCTG PA6 cohort.

Molecular characterization of the MG-GEM groups revealed the association with several KRAS mutations. For example, the proportion of KRAS G12A mutation was significantly higher in the high MG-GEM group, while the proportion of G12V was higher in the low MG-GEM group, in line with their respective association with the prognosis of PDAC patients [38], [39]. Similarly, mutations in SMAD4 were significantly associated with the high MG-GEM group. Previous studies have linked SMAD4 loss to increased glycolysis [40], and drug resistance mediated through lipid accumulation [41] in PDAC.

Over the last decade, several transcriptomic-driven whole-tumor subtype classifications have been published [22], [31], [32], [42], [43], [44], [45], consistently identifying the Classical subtype, associated with better survival outcomes and well-differentiated tumors, and the "Basal-like" subtype, associated with poor prognosis and less-differentiated tumors. When comparing the enrichment of several classifications signatures between the MG-GEM groups, the high MG-GEM group showed a significant association with "Basal-like" and active stroma subtypes. In contrast, the low MG-GEM group was enriched for "Classical" and immune subtypes, both linked to better prognosis. The enrichment of the immune classical subtype within the low MG-GEM group suggests that these tumors may possess a more immunogenic

microenvironment. This molecular phenotype, characterized by both lower glycolytic stress and immune activation, raises the potential for combination strategies involving gemcitabine and immunotherapy in this subgroup. Further study of the immune landscape of low MG-GEM tumors may help refine patient selection for such combined approaches.

GEM treatment seems to be more effective in the “classical” tumors [46]. However, an analysis of the subtypes defined by Puleo et al. within high and low MG-GEM groups, revealed that 6 tumors classified as «Pure Classical» tumors fell within the high MG-GEM group. This suggests that the MG-GEM tool/signature can identify classical tumors that may be resistant to GEM offering a stratification method that is superior to the current molecular subtyping in terms of predicting treatment resistance. MG-GEM score revealed significant differences in OS and DFS among patients treated with GEM. However, no significant differences were observed in patients treated with FFX, emphasizing further the existing connection between MG stress and GEM therapy in PDAC. Furthermore, the higher expression of GEM metabolic blockers CDA and RRM1 genes in high MG-GEM group confirms the specificity of this tool in identifying GEM-resistant populations.

Notably, while GemPred transcriptomic signature has been developed to predict GEM response based on clinical parameters [47], this study demonstrates that MG-GEM signature operates independently of GemPred. Moreover, the prognostic value of MG-GEM across both GemPred-defined patient groups highlights its potential as a metabolically based, predictive independent marker associated with mechanisms of chemoresistance. These findings suggest that combining MG-GEM with GemPred enhances the ability to identify GEM-sensitive and GEM-resistant patients, thereby supporting more effective personalized treatment strategies.

This study has several limitations. First, the use of retrospective cohorts may have resulted in incomplete OS and DFS information, limiting the number of samples available to build the model. From a clinical research perspective, integrating MG-stress status with other predictive biomarkers or DNA molecular profiling data could further enhance the accuracy of the signature. Moreover, testing the signature in the neoadjuvant setting could provide valuable insights into its predictive power and clinical utility in early treatment response. In conclusion, our study established a novel predictive model based on MG-stress, which has been recently brought on the chemoresistance chessboard in various cancers, including colon [17], breast [18], and PDAC [19]. The model, comprising 16 genes, was validated in both independent internal and external cohorts, and demonstrated the ability to distinguish between GEM-resistant and GEM-sensitive PDAC patient groups. The broader clinical application of the MG-GEM model, alone or in combination with GemPred could serve as a valuable tool for predicting GEM chemosensitivity and chemoresistance and propose the potential use of MG scavengers to promote response to GEM treatment and/or immunotherapy in PDAC patients.

Tables

Table 1

Variable	N	Overall N = 85[1]	MG-GEM High Risk N = 43[1]	MG-GEM Low Risk N = 42[1]	p-value[2]
Age	85				0.23
<= 65 years		35 (41%)	15 (35%)	20 (48%)	
>65 years		50 (59%)	28 (65%)	22 (52%)	
Sex	85				0.72
Female		34 (40%)	18 (42%)	16 (38%)	
Male		51 (60%)	25 (58%)	26 (62%)	
Histological grade	83				0.091
G1		27 (33%)	9 (21%)	18 (44%)	
G2		42 (51%)	25 (60%)	17 (41%)	
G3		14 (17%)	8 (19%)	6 (15%)	
Resection Margin	85				0.28
R0		64 (75%)	30 (70%)	34 (81%)	
R1		19 (22%)	11 (26%)	8 (19%)	
R3		2 (2.4%)	2 (4.7%)	0 (0%)	
TNM.Stage	85				0.64
IA		3 (3.5%)	1 (2.3%)	2 (4.8%)	
IB		4 (4.7%)	1 (2.3%)	3 (7.1%)	
IIA		15 (18%)	7 (16%)	8 (19%)	
IIB		63 (74%)	34 (79%)	29 (69%)	
Lymphatic invasion	82	50 (61%)	23 (56%)	27 (66%)	0.37
Perineural invasion	82	62 (76%)	35 (85%)	27 (66%)	**0.040**
Vascular invasion	82	42 (51%)	20 (49%)	22 (54%)	0.66

Variable	N	Overall N = 85[1]	MG-GEM High Risk N = 43[1]	MG-GEM Low Risk N = 42[1]	p-value[2]
Treatment	85				0.43
5FU		2 (2.4%)	1 (2.3%)	1 (2.4%)	
Gemcitabine		54 (64%)	24 (56%)	30 (71%)	
Other		2 (2.4%)	1 (2.3%)	1 (2.4%)	
Untreated		27 (32%)	17 (40%)	10 (24%)	

[1]Median (IQR) or Frequency (%)

[2]Pearson's Chi-squared test; Fisher's exact test

Table1. Clinical Characteristics of the high and low MG-GEM patient groups.

Table 2

Variable	N	Overall N = 85[1]	MG-GEM High Risk N = 43[1]	MG-GEM Low Risk N = 42[1]	p-value[2]
KRAS mutation	62				**0.043**
G12A		29 (47%)	19 (59%)	10 (33%)	
G12V		23 (37%)	7 (22%)	16 (53%)	
wt		10 (16%)	6 (19%)	4 (13%)	
TP53 mutation	78				0.20
nonsense		47 (60%)	27 (68%)	20 (53%)	
wt		29 (37%)	12 (30%)	17 (45%)	
indel_frameshift		1 (1.3%)	1 (2.5%)	0 (0%)	
indel_inframe		1 (1.3%)	0 (0%)	1 (2.6%)	
SMAD4 mutation	78				**0.049**
wt		64 (82%)	29 (73%)	35 (92%)	
indel_frameshift		0 (0%)	0 (0%)	0 (0%)	
nonsense		13 (17%)	10 (25%)	3 (7.9%)	
indel_inframe		1 (1.3%)	1 (2.5%)	0 (0%)	
CDKN2A mutation	78				0.16
wt		63 (81%)	29 (73%)	34 (89%)	
indel_frameshift		6 (7.7%)	5 (13%)	1 (2.6%)	
nonsense		8 (10%)	5 (13%)	3 (7.9%)	
indel_inframe		1 (1.3%)	1 (2.5%)	0 (0%)	
Puleo et al.	77				**<0.001**
Desmoplastic		16 (21%)	10 (25%)	6 (16%)	
Immune Classical		13 (17%)	1 (2.5%)	12 (32%)	
Pure Basal-like		9 (12%)	8 (20%)	1 (2.7%)	
Pure Classical		19 (25%)	6 (15%)	13 (35%)	
Stroma Activated		20 (26%)	15 (38%)	5 (14%)	
Bailey et al.	85				**<0.001**

Variable	N	Overall N = 85[1]	MG-GEM High Risk N = 43[1]	MG-GEM Low Risk N = 42[1]	p-value[2]
ADEX		20 (24%)	8 (19%)	12 (29%)	
Immunogenic		7 (8.2%)	1 (2.3%)	6 (14%)	
Progenitor		25 (29%)	5 (12%)	20 (48%)	
Squamous		33 (39%)	29 (67%)	4 (9.5%)	
Moffit et al. Tumor	85				0.45
Basal		46 (54%)	25 (58%)	21 (50%)	
Classical		39 (46%)	18 (42%)	21 (50%)	
Moffit et al. Stroma	85				**0.014**
Absent		29 (34%)	13 (30%)	16 (38%)	
Activated		47 (55%)	29 (67%)	18 (43%)	
Normal		9 (11%)	1 (2.3%)	8 (19%)	
Purist	77				**0.008**
Basal		16 (21%)	13 (33%)	3 (8.1%)	
Classical		61 (79%)	27 (68%)	34 (92%)	

[1]Median (IQR) or Frequency (%)

[2]Fisher's exact test; Pearson's Chi-squared test

Table2. Molecular characteristics of the high and low MG-GEM patient groups.

Figures

Figure 1

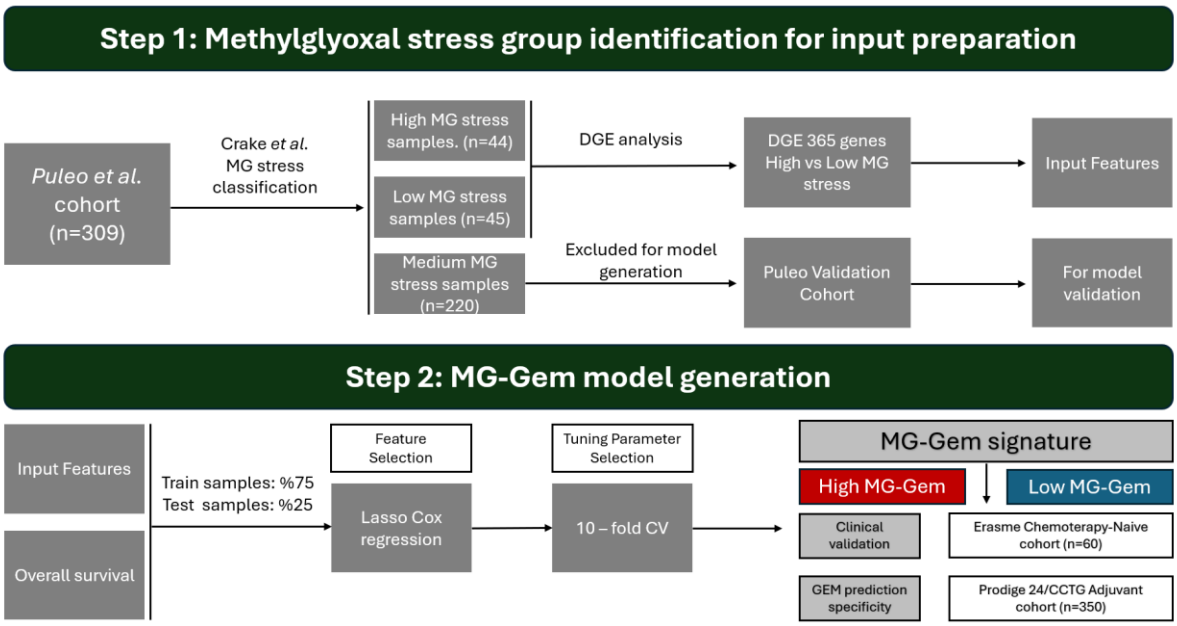

Figure 1. Diagram representing the overall workflow of the study design.

MG: Methylglyoxal; DGE: Differential gene expression; CV: Cross-validation GEM: Gemcitabine.

Figure 2

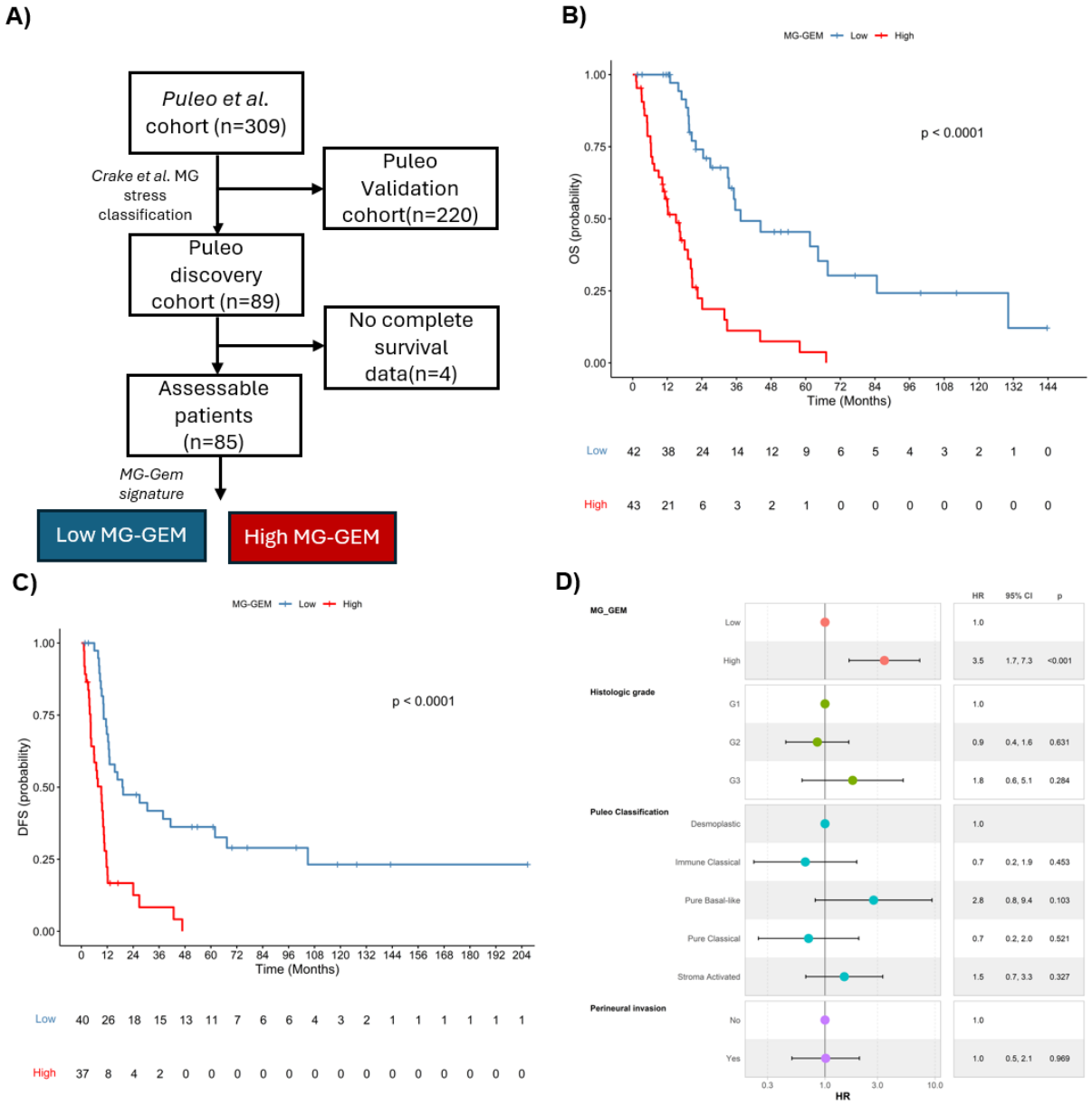
A)
Puleo et al. cohort (n=309)
Crake et al. MG stress classification
Puleo Validation cohort(n=220)
Puleo discovery cohort (n=89)
No complete survival data(n=4)
Assessable patients (n=85)
MG-Gem signature
Low MG-GEM
High MG-GEM
B)
MG-GEM Low High
p < 0.0001
OS (probability)
Time (Months)
Low 42 38 24 14 12 9 6 5 4 3 2 1 0
High 43 21 6 3 2 1 0 0 0 0 0 0 0
C)
MG-GEM Low High
p < 0.0001
DFS (probability)
Time (Months)
Low 40 26 18 15 13 11 7 6 6 4 3 2 1 1 1 1 1
High 37 8 4 2 0 0 0 0 0 0 0 0 0 0 0 0 0
D)
HR 95% CI p
MG_GEM
Low 1.0
High 3.5 1.7, 7.3 <0.001
Histologic grade
G1 1.0
G2 0.9 0.4, 1.6 0.631
G3 1.8 0.6, 5.1 0.284
Puleo Classification
Desmoplastic 1.0
Immune Classical 0.7 0.2, 1.9 0.453
Pure Basal-like 2.8 0.8, 9.4 0.103
Pure Classical 0.7 0.2, 2.0 0.521
Stroma Activated 1.5 0.7, 3.3 0.327
Perineural invasion
No 1.0
Yes 1.0 0.5, 2.1 0.969
HR

Figure 2. Survival analysis confirming the prognostic significance of MG-GEM stratification in the Puleo discovery cohort (n=89).

(A) Discovery cohort flowchart.

(B,C) Visualization of Kaplan-Meier analysis of OS and DFS.

(D) Forest plot showing the stratified multivariate Cox hazard regression including the MG-GEM groups.

MG: Methylglyoxal; GEM: Gemcitabine; OS: Overall Survival; DFS: Disease Free Survival; HR: Hazard Ratio; CI: Confidence Interval.

Figure 3

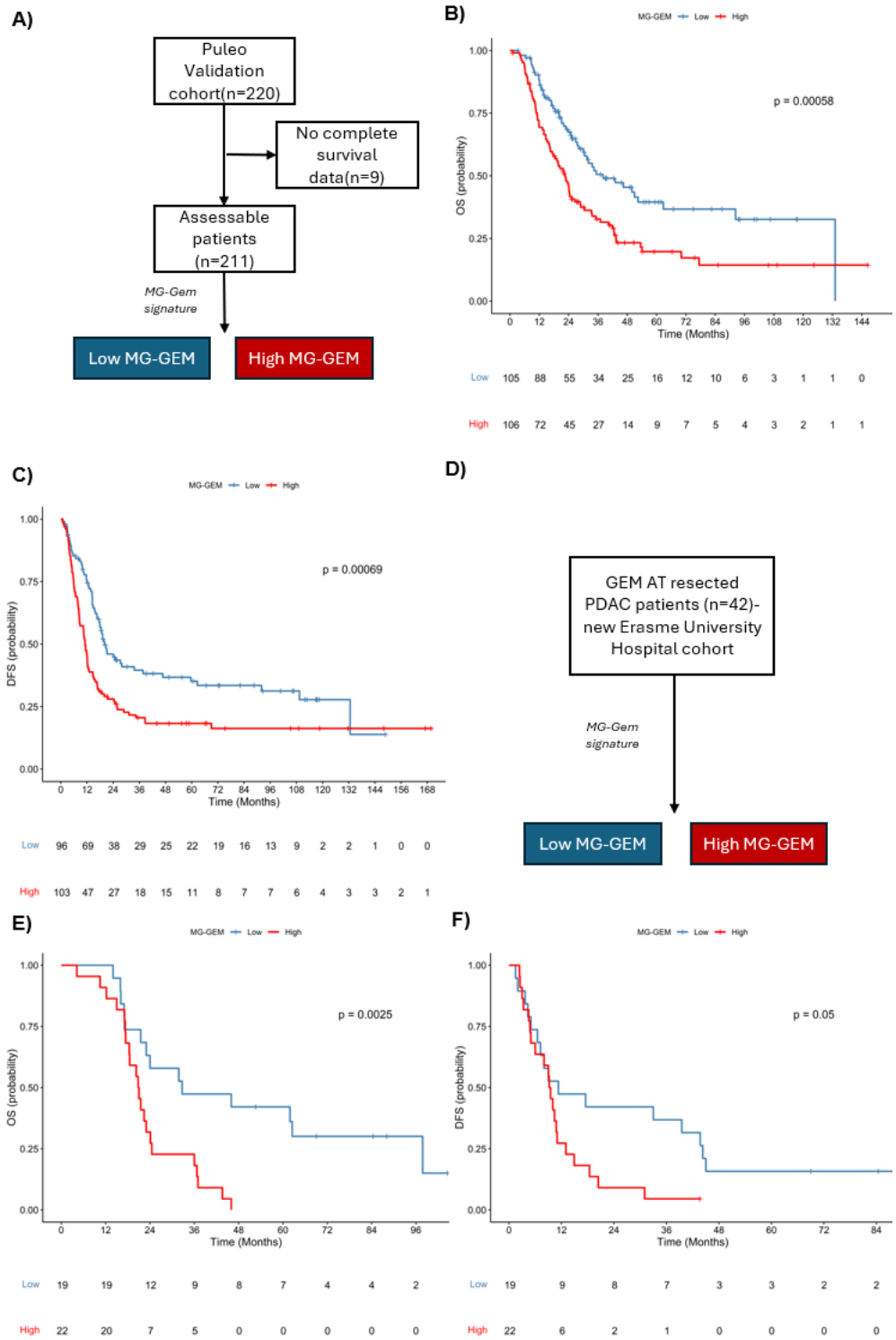
A)
Puleo Validation cohort(n=220)
No complete survival data(n=9)
Assessable patients (n=211)
MG-Gem signature
Low MG-GEM
High MG-GEM
B)
MG-GEM Low High
p = 0.00058
OS (probability)
Time (Months)
Low 105 88 55 34 25 16 12 10 6 3 1 1 0
High 106 72 45 27 14 9 7 5 4 3 2 1 1
C)
MG-GEM Low High
p = 0.00069
DFS (probability)
Time (Months)
Low 96 69 38 29 25 22 19 16 13 9 2 2 1 0 0
High 103 47 27 18 15 11 8 7 7 6 4 3 3 2 1
D)
GEM AT resected PDAC patients (n=42)- new Erasme University Hospital cohort
MG-Gem signature
Low MG-GEM
High MG-GEM
E)
MG-GEM Low High
p = 0.0025
OS (probability)
Time (Months)
Low 19 19 12 9 8 7 4 4 2
High 22 20 7 5 0 0 0 0 0
F)
MG-GEM Low High
p = 0.05
DFS (probability)
Time (Months)
Low 19 9 8 7 3 3 2 2
High 22 6 2 1 0 0 0 0

Figure 3. Survival analyses validating the prognostic value of MG-GEM stratification.

(A) Puleo Validation cohort (n=220) flowchart.

(B,C) Significantly worse OS and DFS observed in High MG- GEM group in Kaplan-Meier analysis in the Puleo Validation cohort.

(D) GEM AT resected PDAC patients, Erasme University Hospital cohort (n=42) flowchart.

(E,F) Significantly worse OS and DFS observed in High MG- GEM group in Kaplan-Meier analysis in the chemotherapy-naive Erasme University Hospital cohort.

MG: Methylglyoxal; OS: Overall Survival; DFS: Disease Free Survival.

Figure 4

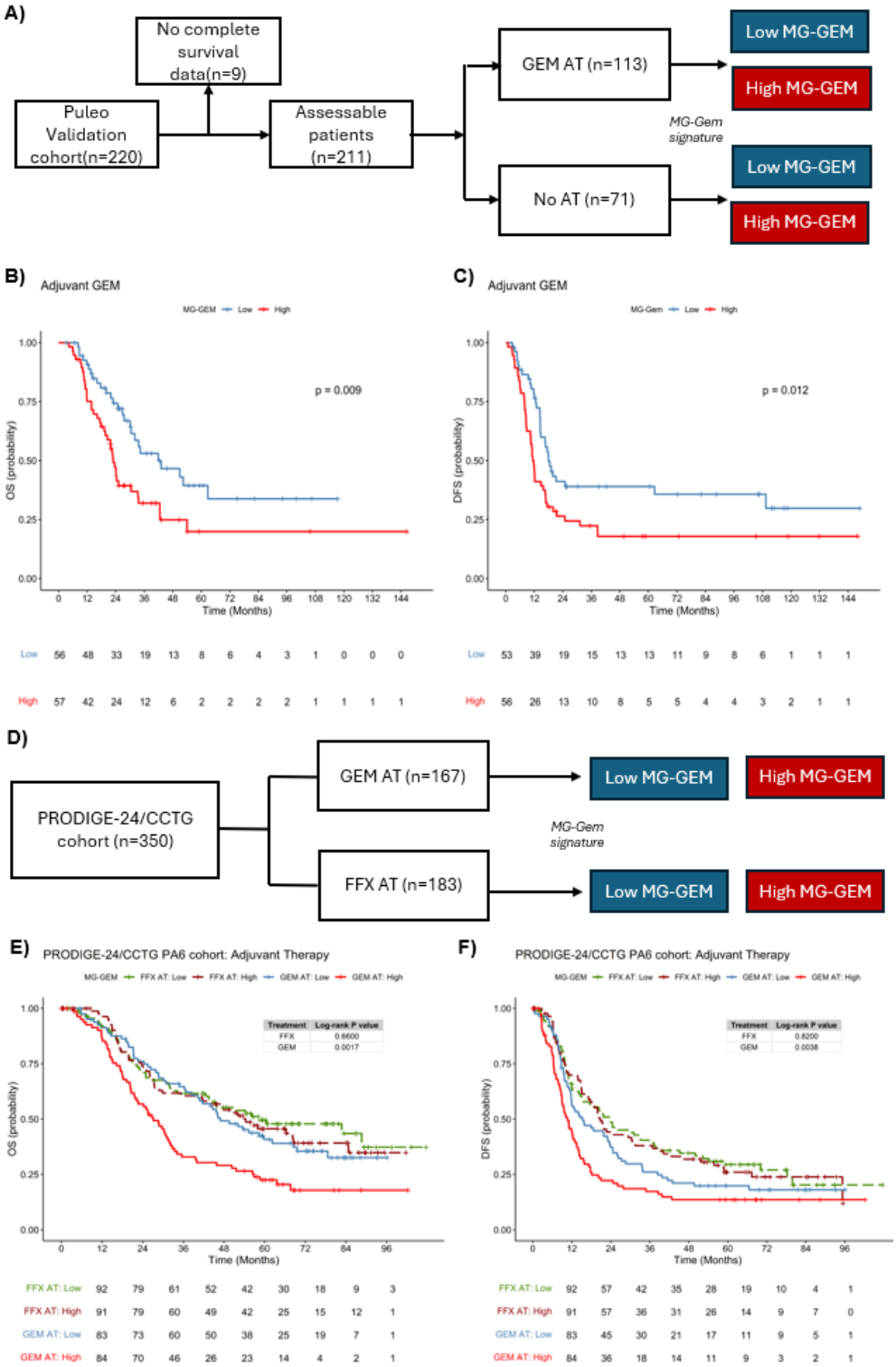
A)
No complete survival data(n=9)
Puleo Validation cohort(n=220)
Assessable patients (n=211)
GEM AT (n=113)
No AT (n=71)
MG-Gem signature
Low MG-GEM
High MG-GEM
Low MG-GEM
High MG-GEM
B) Adjuvant GEM
MG-GEM Low High
p = 0.009
OS (probability)
Time (Months)
Low 56 48 33 19 13 8 6 4 3 1 0 0 0
High 57 42 24 12 6 2 2 2 2 1 1 1 1
C) Adjuvant GEM
MG-Gem Low High
p = 0.012
DFS (probability)
Time (Months)
Low 53 39 19 15 13 13 11 9 8 6 1 1 1
High 56 26 13 10 8 5 5 4 4 3 2 1 1
D)
PRODIGE-24/CCTG cohort (n=350)
GEM AT (n=167)
FFX AT (n=183)
MG-Gem signature
Low MG-GEM
High MG-GEM
Low MG-GEM
High MG-GEM
E) PRODIGE-24/CCTG PA6 cohort: Adjuvant Therapy
MG-GEM FFX AT: Low FFX AT: High GEM AT: Low GEM AT: High
Treatment Log-rank P value
FFX 0.6600
GEM 0.0017
OS (probability)
Time (Months)
FFX AT: Low 92 79 61 52 42 30 18 9 3
FFX AT: High 91 79 60 49 42 25 15 12 1
GEM AT: Low 83 73 60 50 38 25 19 7 1
GEM AT: High 84 70 46 26 23 14 4 2 1
F) PRODIGE-24/CCTG PA6 cohort: Adjuvant Therapy
MG-GEM FFX AT: Low FFX AT: High GEM AT: Low GEM AT: High
Treatment Log-rank P value
FFX 0.8200
GEM 0.0038
DFS (probability)
Time (Months)
FFX AT: Low 92 57 42 35 28 19 10 4 1
FFX AT: High 91 57 36 31 26 14 9 7 0
GEM AT: Low 83 45 30 21 17 11 9 5 1
GEM AT: High 84 36 18 14 11 9 3 2 1

Figure 4. MG-GEM specifically predicts response to GEM therapy but not to FFX.

(A) Puleo Validation cohort flowchart stratified by the type of adjuvant treatment.

(B, C) Significantly worse OS and DFS observed in High MG- GEM group in Kaplan-Meier analysis in the adjuvant GEM receiving Puleo Validation cohort population.

(D) PRODIGE 24/CCTG PA6 cohort flowchart.

(E,F) Patients from the PRODIGE 24/CCTG PA6 study stratified as High MG-GEM and receiving adjuvant GEM (red curve) showed significantly poorer overall survival (OS) and disease-free survival (DFS) compared to low MG-GEM patient's group (blue curve) according to Kaplan-Meier analysis. These differences were not significant for patients that received FFX as adjuvant treatment (brown and green curves)

MG: Methylglyoxal; OS: overall survival; DFS: Disease Free Survival; AT: Adjuvant therapy; GEM: Gemcitabine; FFX: Folfirinox.

Figure 5

A)

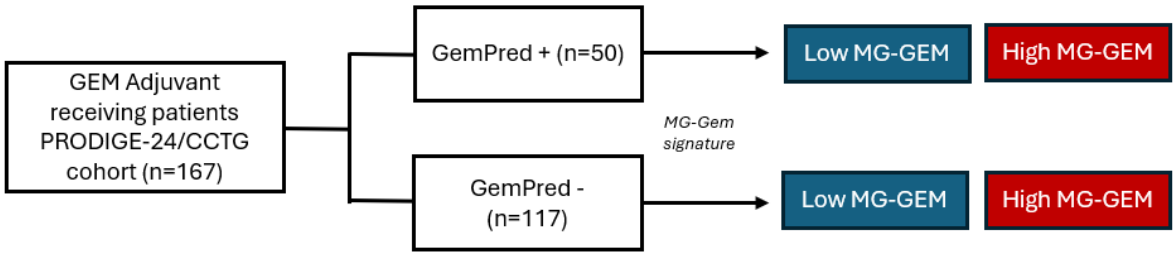

B)

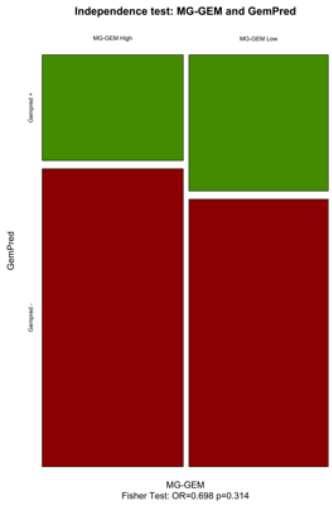

C)

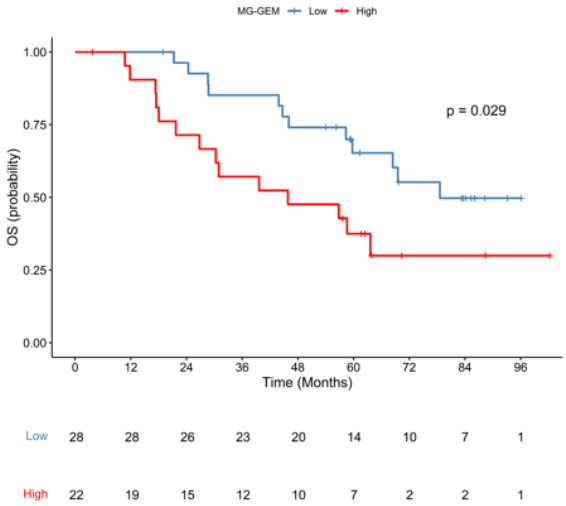

D)

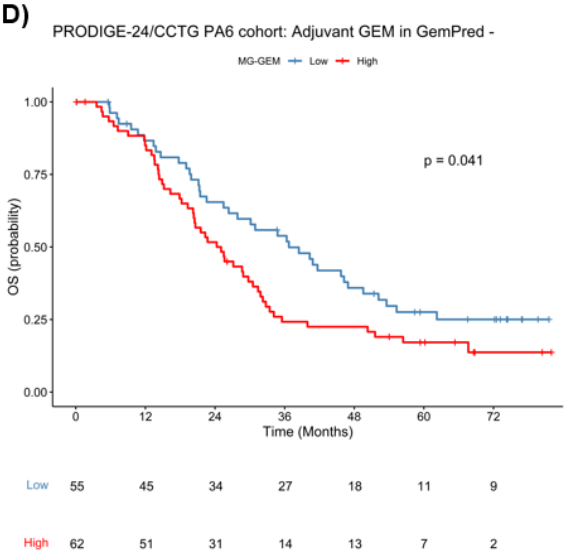

Figure 5. Independent Validation and Integration of MG-GEM and GemPred signatures

(A) GEM-adjuvant PRODIGE-24/CCTG PA6/ cohort stratified per GemPred groups individual flowcharts.

(B) Fisher test of independence between the MG-GEM and GemPred groups in the samples treated with adjuvant Gemcitabine in the PRODIGE-24/CCTG PA6 cohort.

(C,D) Significantly worse OS observed in High MG-GEM group in Kaplan-Meier analysis in the adjuvant GEM receiving PRODIGE-24/CCTG PA6 cohort population in the GemPred+ group (C) and GemPred- group (D).

OS: Overall Survival; MG: Methylglyoxal; AT: Adjuvant therapy; GEM: Gemcitabine.

Supplementary Tables

Suppl Table 1

Genes	Regression Coefficients
FAM162A	0.012505829
SEC61G	0.012247897
NT5E	0.061947891
TREM1	0.006879062
SLC3A1	-0.134238750
CALB2	0.163784593
TFF1	-0.020302925
SLC11A1	0.310568838
PDIA2	0.309967832
PADI1	0.206518361
ADH1C	-0.044073847
FXYD3	-0.256065865
SCEL	0.244610176
ECT2	-0.046611035
TIPARP	0.014119270
IGHG1	-0.135090509

Supplementary table 1. The lasso cox regression coefficients of the 16 genes (FAM162A, SEC61G, NT5E, TREM1, SLC3A1, CALB2, TFF1, SLC11A1, PDIA2, PADI1, ADH1C, FXYD3, SCEL, ECT2, TIPARP and IGHG1) used, in combination with the expression level of each gene, to calculate the final MG-GEM.

Supplementary Figures

Supp Figure 1

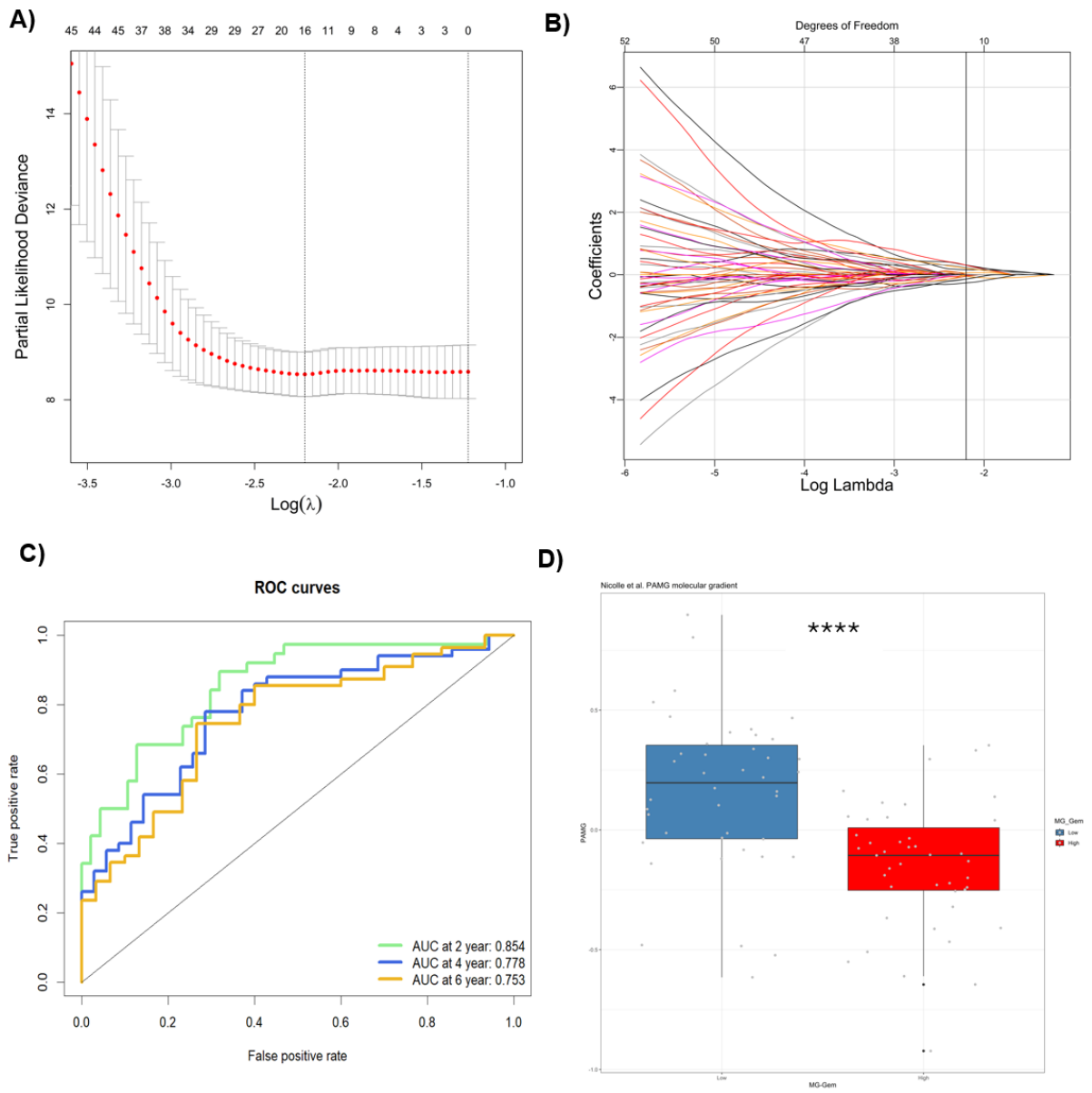

Supplementary Figure 1. Feature selection with the logistic Lasso cox regression model by 10-fold cross-validation, the minimum criterion and the model evaluation.

(A) Lasso coefficients of Lasso cox regression model.

(B) Coefficient profile plot against the log (lambda) sequence.

(C) A comparison of the ROC curves for the risk score with arbitrary time cuts.

(D) A continuous gradient of PDAC pre-existing classifications PAMG was applied in the discovery cohort, showing a significantly higher molecular gradient PAMG score in favor of the Low MG-GEM score.

AUC: Area under the curve.

Supp Figure 2

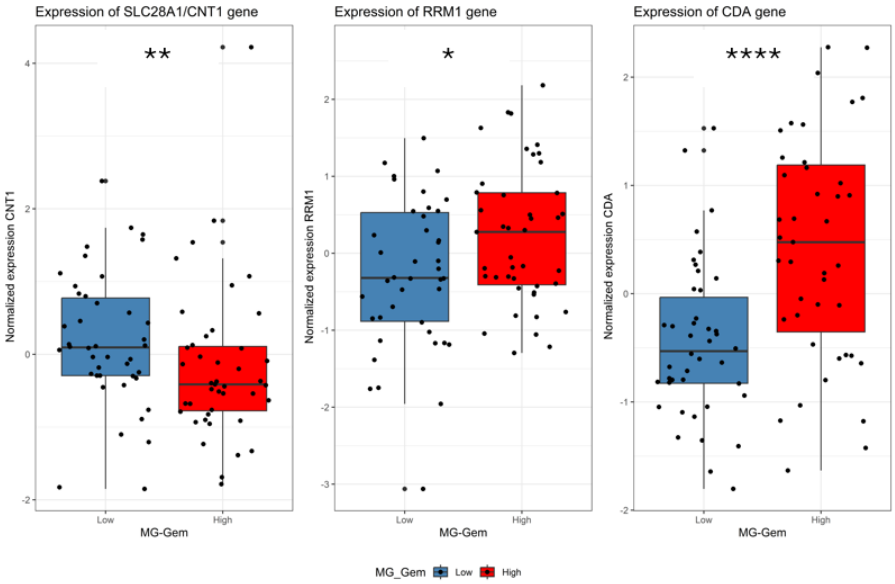

Supplementary Figure 2. Expression of the genes related to the GEM transport and metabolism in high and low MG-GEM groups. The low MG-GEM group showed higher expression levels of the GEM transporter CNT1, a transporter for GEM uptake (p=0.0099). In contrast, the high MG-GEM group showed elevated expression of two enzymes associated with GEM resistance: RRM1 (p=0.047), and CDA (p=4.9e-05).

CNT1: Concentrative nucleoside transporter 1 RRM1: ribonucleotide reductase catalytic subunit M1 CDA: cytidine deaminase.

Supp Figure 3

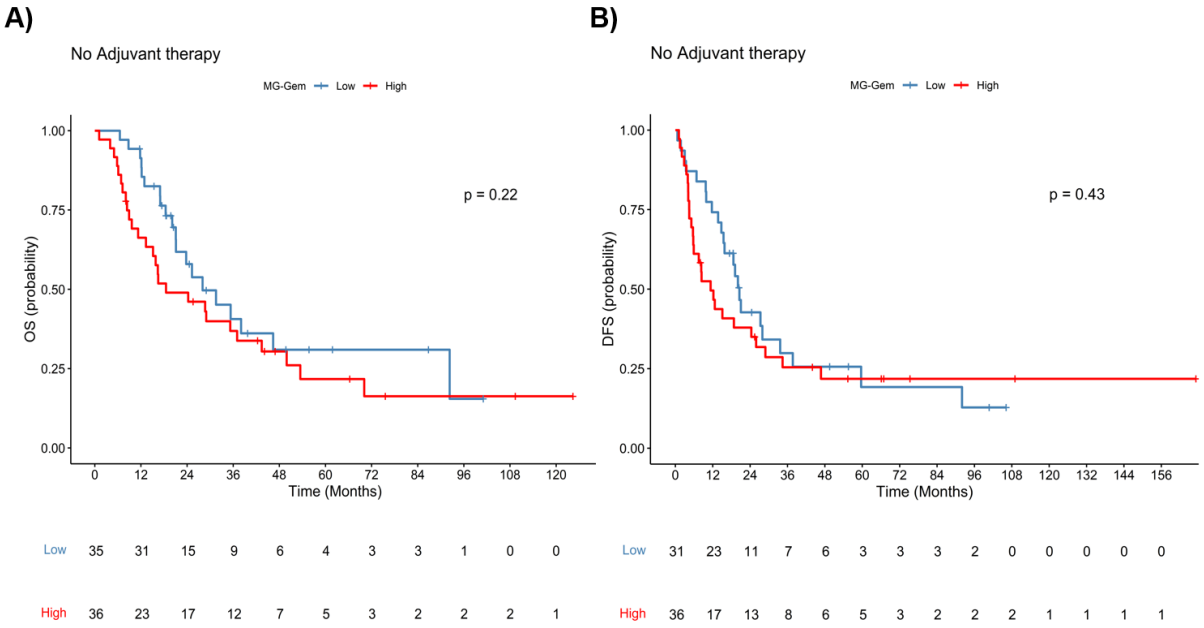

Supplementary Figure 3. OS and DFS results of the combination of MG-GEM and GemPred transcriptomics signature.

(A,B) No significant OS (A) and DFS (B) differences observed between MG-GEM groups in Kaplan-Meier analysis in the no adjuvant treatment patients.

Kaplan-Meier analysis showed no significant OS (A) or DFS (B) differences in the MG-GEM high group among patients without adjuvant treatment in the Puleo validation cohort. MG: Methylglyoxal; DFS: Disease Free Survival; AT: Adjuvant therapy; GEM: Gemcitabine.

Supp Figure 4

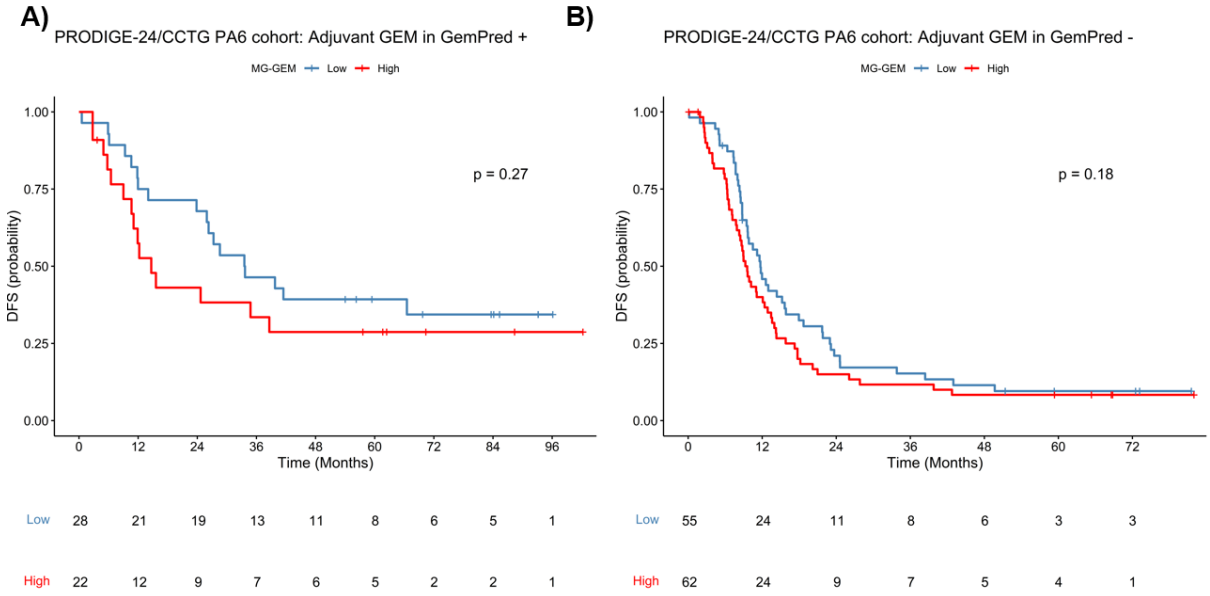

Supplementary Figure 4. DFS results of the combination of MG-GEM and GemPred transcriptomics signature.

(A,B) No significant DFS differences observed in High MG-GEM group in Kaplan-Meier analysis in the adjuvant GEM receiving PRODIGE-24/CCTG cohort population in the GemPred+ group (A) and GemPred- group (B).

DFS: Disease Free Survival, MG: Methylglyoxal; AT: Adjuvant therapy; GEM: Gemcitabine.

References

[1] L. Rahib, B. D. Smith, R. Aizenberg, A. B. Rosenzweig, J. M. Fleshman, and L. M. Matrisian, 'Projecting cancer incidence and deaths to 2030: The unexpected burden of thyroid, liver, and pancreas cancers in the united states', Jun. 01, 2014, *American Association for Cancer Research Inc.* doi: 10.1158/0008-5472.CAN-14-0155.

[2] M. Dalmartello *et al.*, 'European cancer mortality predictions for the year 2022 with focus on ovarian cancer', *Annals of Oncology*, vol. 33, no. 3, pp. 330–339, Mar. 2022, doi: 10.1016/j.annonc.2021.12.007.

[3] T. Conroy *et al.*, 'FOLFIRINOX or Gemcitabine as Adjuvant Therapy for Pancreatic Cancer', *New England Journal of Medicine*, vol. 379, no. 25, pp. 2395–2406, Dec. 2018, doi: 10.1056/nejmoa1809775.

[4] M. A. Tempero *et al.*, 'Adjuvant nab-Paclitaxel 1 Gemcitabine in Resected Pancreatic Ductal Adenocarcinoma: Results From a Randomized, Open-Label, Phase III Trial', *J Clin Oncol*, vol. 41, pp. 2007–2019, 2022, doi: 10.1200/JCO.22.

[5] Z. A. Wainberg *et al.*, 'NALIRIFOX versus nab-paclitaxel and gemcitabine in treatment-naive patients with metastatic pancreatic ductal adenocarcinoma (NAPOLI 3): a randomised, open-label, phase 3 trial', *The Lancet*, vol. 402, no. 10409, pp. 1272–1281, Oct. 2023, doi: 10.1016/S0140-6736(23)01366-1.

[6] S. Benkhaled *et al.*, 'Combination, Modulation and Interplay of Modern Radiotherapy with the Tumor Microenvironment and Targeted Therapies in Pancreatic Cancer: Which Candidates to Boost Radiotherapy?', Feb. 01, 2023, *MDPI*. doi: 10.3390/cancers15030768.

[7] M. Hilmi *et al.*, 'The immunological landscape in pancreatic ductal adenocarcinoma and overcoming resistance to immunotherapy', *Lancet Gastroenterol Hepatol*, vol. 8, no. 12, pp. 1129–1142, 2023, doi: https://doi.org/10.1016/S2468-1253(23)00207-8.

[8] A. Lambert *et al.*, 'An update on treatment options for pancreatic adenocarcinoma', 2019, *SAGE Publications Inc.* doi: 10.1177/1758835919875568.

[9] R. Maréchal *et al.*, 'Levels of Gemcitabine Transport and Metabolism Proteins Predict Survival Times of Patients Treated With Gemcitabine for Pancreatic Adenocarcinoma', *Gastroenterology*, vol. 143, no. 3, pp. 664-674.e6, 2012, doi: https://doi.org/10.1053/j.gastro.2012.06.006.

[10] R. Nicolle *et al.*, 'A transcriptomic signature to predict adjuvant gemcitabine sensitivity in pancreatic adenocarcinoma', *Annals of Oncology*, vol. 32, no. 2, pp. 250–260, Feb. 2021, doi: 10.1016/j.annonc.2020.10.601.

[11] R. Nicolle *et al.*, 'Prediction of Adjuvant Gemcitabine Sensitivity in Resectable Pancreatic Adenocarcinoma Using the GemPred RNA Signature: An Ancillary Study of the PRODIGE-

24/CCTG PA6 Clinical Trial', *Journal of Clinical Oncology*, vol. 42, no. 9, pp. 1067–1076, Mar. 2024, doi: 10.1200/JCO.22.02668.

[12] S. K. Shukla *et al.*, 'MUC1 and HIF-1alpha Signaling Crosstalk Induces Anabolic Glucose Metabolism to Impart Gemcitabine Resistance to Pancreatic Cancer', *Cancer Cell*, vol. 32, no. 1, pp. 71-87.e7, Jul. 2017, doi: 10.1016/j.ccell.2017.06.004.

[13] Y. Xi, P. Yuan, T. Li, M. Zhang, M. F. Liu, and B. Li, 'hENT1 reverses chemoresistance by regulating glycolysis in pancreatic cancer', *Cancer Lett*, vol. 479, pp. 112–122, Jun. 2020, doi: 10.1016/j.canlet.2020.03.015.

[14] S. Dai *et al.*, 'Glycolysis promotes the progression of pancreatic cancer and reduces cancer cell sensitivity to gemcitabine', *Biomedicine and Pharmacotherapy*, vol. 121, Jan. 2020, doi: 10.1016/j.biopha.2019.109521.

[15] S. A. PHILLIPS and P. J. THORNALLEY, 'The formation of methylglyoxal from triose phosphates', *Eur J Biochem*, vol. 212, no. 1, pp. 101–105, Feb. 1993, doi: https://doi.org/10.1111/j.1432-1033.1993.tb17638.x.

[16] C. G. Schalkwijk and C. D. A. Stehouwer, 'Methylglyoxal, a Highly Reactive Dicarbonyl Compound, in Diabetes, Its Vascular Complications, and Other Age-Related Diseases', *Physiol Rev*, vol. 100, no. 1, pp. 407–461, Sep. 2019, doi: 10.1152/physrev.00001.2019.

[17] B. Chiavarina *et al.*, 'Methylglyoxal-mediated stress correlates with high metabolic activity and promotes tumor growth in colorectal cancer', *Int J Mol Sci*, vol. 18, no. 1, Jan. 2017, doi: 10.3390/ijms18010213.

[18] M. J. Nokin *et al.*, 'Methylglyoxal, a glycolysis metabolite, triggers metastasis through MEK/ERK/SMAD1 pathway activation in breast cancer', *Breast Cancer Research*, vol. 21, no. 1, Jan. 2019, doi: 10.1186/s13058-018-1095-7.

[19] R. Crake *et al.*, 'Resistance to Gemcitabine in Pancreatic Cancer Is Connected to Methylglyoxal Stress and Heat Shock Response', *Cells*, vol. 12, no. 10, May 2023, doi: 10.3390/cells12101414.

[20] J. Bellier *et al.*, 'Methylglyoxal Scavengers Resensitize KRAS-Mutated Colorectal Tumors to Cetuximab', *Cell Rep*, vol. 30, no. 5, pp. 1400-1416.e6, Feb. 2020, doi: 10.1016/j.celrep.2020.01.012.

[21] M. J. Nokin *et al.*, 'Hormetic potential of methylglyoxal, a side-product of glycolysis, in switching tumours from growth to death', *Sci Rep*, vol. 7, no. 1, Dec. 2017, doi: 10.1038/s41598-017-12119-7.

[22] F. Puleo *et al.*, 'Stratification of Pancreatic Ductal Adenocarcinomas Based on Tumor and Microenvironment Features', *Gastroenterology*, vol. 155, no. 6, pp. 1999-2013.e3, Dec. 2018, doi: 10.1053/j.gastro.2018.08.033.

[23] C. Bouchart *et al.*, 'Favorable histo-molecular remodeling of pancreatic ductal adenocarcinoma after Total Neoadjuvant Therapy including Stereotactic Body

Radiotherapy', *bioRxiv*, p. 2024.04.30.591890, Jan. 2024, doi: 10.1101/2024.04.30.591890.

[24] T. Conroy *et al.*, 'Five-Year Outcomes of FOLFIRINOX vs Gemcitabine as Adjuvant Therapy for Pancreatic Cancer', *JAMA Oncol*, vol. 8, no. 11, p. 1571, Nov. 2022, doi: 10.1001/jamaoncol.2022.3829.

[25] D. J. McCarthy, Y. Chen, and G. K. Smyth, 'Differential expression analysis of multifactor RNA-Seq experiments with respect to biological variation', *Nucleic Acids Res*, vol. 40, no. 10, pp. 4288–4297, May 2012, doi: 10.1093/nar/gks042.

[26] M. E. Ritchie *et al.*, 'Limma powers differential expression analyses for RNA-sequencing and microarray studies', *Nucleic Acids Res*, vol. 43, no. 7, p. e47, Jan. 2015, doi: 10.1093/nar/gkv007.

[27] R. Nicolle *et al.*, 'Establishment of a pancreatic adenocarcinoma molecular gradient (PAMG) that predicts the clinical outcome of pancreatic cancer', *EBioMedicine*, vol. 57, Jul. 2020, doi: 10.1016/j.ebiom.2020.102858.

[28] J. Friedman, T. Hastie, and R. Tibshirani, 'Regularization Paths for Generalized Linear Models via Coordinate Descent', 2010. [Online]. Available: http://www.jstatsoft.org/

[29] G. Sturm *et al.*, 'Comprehensive evaluation of transcriptome-based cell-type quantification methods for immuno-oncology', in *Bioinformatics*, Oxford University Press, Jul. 2019, pp. i436–i445. doi: 10.1093/bioinformatics/btz363.

[30] E. Becht *et al.*, 'Estimating the population abundance of tissue-infiltrating immune and stromal cell populations using gene expression', *Genome Biol*, vol. 17, no. 1, Oct. 2016, doi: 10.1186/s13059-016-1070-5.

[31] R. A. Moffitt *et al.*, 'Virtual microdissection identifies distinct tumor- and stroma-specific subtypes of pancreatic ductal adenocarcinoma', *Nat Genet*, vol. 47, no. 10, pp. 1168–1178, Sep. 2015, doi: 10.1038/ng.3398.

[32] P. Bailey *et al.*, 'Genomic analyses identify molecular subtypes of pancreatic cancer', *Nature*, vol. 531, no. 7592, pp. 47–52, Mar. 2016, doi: 10.1038/nature16965.

[33] J. P. Neoptolemos *et al.*, 'Adjuvant Chemotherapy With Fluorouracil Plus Folinic Acid vs Gemcitabine Following Pancreatic Cancer Resection: A Randomized Controlled Trial', *JAMA*, vol. 304, no. 10, pp. 1073–1081, Sep. 2010, doi: 10.1001/jama.2010.1275.

[34] J. M. Karasinska *et al.*, 'Altered gene expression along the glycolysis–cholesterol synthesis axis is associated with outcome in pancreatic cancer', *Clinical Cancer Research*, vol. 26, no. 1, pp. 135–146, Jan. 2020, doi: 10.1158/1078-0432.CCR-19-1543.

[35] A. Daemen *et al.*, 'Metabolite profiling stratifies pancreatic ductal adenocarcinomas into subtypes with distinct sensitivities to metabolic inhibitors', *Proc Natl Acad Sci U S A*, vol. 112, no. 32, pp. E4410–E4417, Aug. 2015, doi: 10.1073/pnas.1501605112.

[36] H. Ying *et al.*, 'Oncogenic kras maintains pancreatic tumors through regulation of anabolic glucose metabolism', *Cell*, vol. 149, no. 3, pp. 656–670, Apr. 2012, doi: 10.1016/j.cell.2012.01.058.

[37] Y. Rong *et al.*, 'Lactate dehydrogenase A is overexpressed in pancreatic cancer and promotes the growth of pancreatic cancer cells', *Tumor Biology*, vol. 34, no. 3, pp. 1523–1530, 2013, doi: 10.1007/s13277-013-0679-1.

[38] M. Minarik, T. Halkova, B. Belsanova, B. Bunganic, M. Zavoral, and L. Benesova, 'Abstract 4943: Detection of specific KRAS mutation type, Gly12Asp (GGT>GAT), in EUS-guided fine needle aspiration cytology (EUS-FNAC) identifies pancreatic cancer patients with poor prognosis', *Cancer Res*, vol. 76, no. 14_Supplement, p. 4943, Jul. 2016, doi: 10.1158/1538-7445.AM2016-4943.

[39] B. Ardalan *et al.*, 'Distinct Molecular and Clinical Features of Specific Variants of KRAS Codon 12 in Pancreatic Adenocarcinoma', *Clinical Cancer Research*, vol. 31, no. 6, pp. 1082–1090, Mar. 2025, doi: 10.1158/1078-0432.CCR-24-3149.

[40] C. Liang *et al.*, 'Localisation of PGK1 determines metabolic phenotype to balance metastasis and proliferation in patients with SMAD4-negative pancreatic cancer', *Gut*, vol. 69, no. 5, p. 888, May 2020, doi: 10.1136/gutjnl-2018-317163.

[41] Y. Wang *et al.*, 'KDM5B promotes SMAD4 loss-driven drug resistance through activating DLG1/YAP to induce lipid accumulation in pancreatic ductal adenocarcinoma', *Cell Death Discov*, vol. 10, no. 1, Dec. 2024, doi: 10.1038/s41420-024-02020-4.

[42] E. A. Collisson *et al.*, 'Subtypes of pancreatic ductal adenocarcinoma and their differing responses to therapy', *Nat Med*, vol. 17, no. 4, pp. 500–503, Apr. 2011, doi: 10.1038/nm.2344.

[43] S. Martens *et al.*, 'Different shades of pancreatic ductal adenocarcinoma, different paths towards precision therapeutic applications', *Annals of Oncology*, vol. 30, no. 9, pp. 1428–1436, Sep. 2019, doi: 10.1093/annonc/mdz181.

[44] M. Chan-Seng-Yue *et al.*, 'Transcription phenotypes of pancreatic cancer are driven by genomic events during tumor evolution', *Nat Genet*, vol. 52, no. 2, pp. 231–240, Feb. 2020, doi: 10.1038/s41588-019-0566-9.

[45] W. L. Hwang *et al.*, 'Single-nucleus and spatial transcriptome profiling of pancreatic cancer identifies multicellular dynamics associated with neoadjuvant treatment', *Nat Genet*, vol. 54, no. 8, pp. 1178–1191, Aug. 2022, doi: 10.1038/s41588-022-01134-8.

[46] H. Singh *et al.*, 'Clinical and Genomic Features of Classical and Basal Transcriptional Subtypes in Pancreatic Cancer', *Clinical Cancer Research*, vol. 30, no. 21, pp. 4932–4942, Nov. 2024, doi: 10.1158/1078-0432.CCR-24-1164.

[47] N. Fraunhoffer *et al.*, 'Development and validation of AI-assisted transcriptomic signatures to personalize adjuvant chemotherapy in patients with pancreatic ductal adenocarcinoma', *Annals of Oncology*, Jun. 2024, doi: 10.1016/j.annonc.2024.06.010.

CORRESPONDING AUTHOR

Oier Azurmendi Senar, Laboratory of Experimental Gastroenterology, Université Libre de Bruxelles, Route de Lennik 808, 1070 Brussels, Belgium, e-mail : oier.azurmendi@ulb.be.

SUPPORT

This study was supported by a collaborative grant from the belgian National Fund for Scientific Research (FNRS) grant awarded to A.B. and J.-L.V.L. (PDR T0011.22). A.B. research is funded by grants from the FNRS, the University of Liège, and “Fondation Léon Fredericq”.VD was supported by the Fondation Belge contre le cancer fundamental research grant FCC 2020-072, FNRS crédit de recherche J.0068.22 and a ULB advanced ARC grant. C.B. research was supported by “Les Amis de l’Institut Bordet / L’Association Jules Bordet” [2024-20] grant.

PRODIGE-24/CCTG PA6 was sponsored by R&D Unicancer and supported by “La Ligue, L’Institut National du Cancer (INCa), and CHUGAI Pharma France” . MOSAPAC was funded by “L’Institut National du Cancer (INCa)» and « La Direction Générale de l’Offre de Soins ”.

DATA SHARING STATEMENT

The datasets that support the findings of this study are not publicly available. Access to the dataset will be granted upon reasonable request sent to the corresponding author (OAS) and Unicancer.

AUTHOR CONTRIBUTIONS :

Conception and design:

Oier Azurmendi Senar, Akeila Bellahcène, Tatjana Arsenijevic, Jean-Luc Van-Laethem.

Financial support:

Akeila Bellahcène, Jean-Luc Van-Laethem.

Administrative support:

Marjorie Mauduit, Tatjana Arsenijevic.

Provision of study materials or patients:

Christelle Bouchart, Julie Navez, Thierry Conroy, Jérome Cros, Jean-Luc Van-Laethem.

Collection and assembly of data:

Kosta Stosic, Jawad Tarfouss, Laurine Verset, Tatjana Arsenijevic.

Data analysis and interpretation:

Oier Azurmendi Senar, Rémy Nicolle, Vincent Detours, Tatjana Arsenijevic.

Manuscript writing: All authors

Final approval of manuscript: All authors

Accountable for all aspects of the work: All authors

AUTHORS' DISCLOSURES OF POTENTIAL CONFLICTS OF INTEREST

No other potential conflicts of interest were reported.